Desalination and Water Treatment
www.deswater.com
doi: 10.1080/19443994.2014.908147

54 (2015) 3358–3371
June

Taylor & Francis
Taylor & Francis Group

Removal of Cr(VI) from aqueous solution on seeds of *Artimisia absinthium* (novel plant material)

Rifaqat Ali Khan Rao[a,*], Shaista Ikram[a], Mohammad Kashif Uddin[b]

[a]*Faculty of Engineering and Technology, Environmental Research Laboratory, Department of Applied Chemistry, Aligarh Muslim University, Aligarh, U.P 202002, India, Tel. +91 0571 2703167, Ext. 3000; email: rakrao1@rediffmail.com*
[b]*Basic Engineering Sciences Department, College of Engineering, Majmaah University, Al-Majmaah, Kingdom of Saudi Arabia*

Received 12 November 2013; Accepted 19 March 2014

ABSTRACT

Artimisia absinthium, a medicinal plant material, showed excellent adsorption in removing mutagenic Cr(VI) from aqueous solution along with Cu(II), Ni(II), and Zn(II). Various parameters like effect of pH, contact time, temperature, and initial concentration were investigated using batch process to optimize conditions for maximum adsorption. *A. absinthium* was characterized using scanning electron microscopy (SEM). Adsorption of Cr(VI) was favorable at pH 2 as 96% of Cr(VI) could be removed from aqueous solution. However, adsorption of Cr(VI) decreased to 73% in presence of electrolyte (0.1 N KNO_3) at pH 2. The point of zero charge of *A. absinthium* was 3.9 in double distilled water. The adsorption data were analyzed using Langmuir, Freundlich, Temkin, Hasley, and Dubinin–Redushkeuich isotherm models at 30, 40, and 50°C. The maximum monolayer adsorption capacity towards Cr(VI) was found to be 46.99 mg g^{-1} at 30°C which was relatively large compared to some other similar adsorbents reported earlier. The kinetic data showed that pseudo-second-order rate equation was better obeyed than pseudo-first-order. The intra-particle diffusion model showed that Cr(VI) adsorption involved three different stages. The breakthrough and exhaustive capacities of the adsorbent were found to be 35 and 45 mg g^{-1}, respectively, at pH 2. Desorption study showed that 93.05% Cr(VI) could be desorbed by column operation with 0.01 N NaOH solution.

Keywords: Artimisia absinthium; Adsorption; Cr(VI); Isotherms; Kinetics

1. Introduction

One of the serious threats to our fascinating and fragile environment is the discharge of untreated effluent into the water bodies. Among the various contaminants, discharge of heavy metal ions into the water bodies are of prime concern because of their persistent nature, toxicity, and subsequent bio-accumulation leading to ecological problems [1]. In the array of heavy metal ions, chromium is of special interest because it is an essential nutrient as well as a carcinogen [2]. Dietary deficiency of chromium (III) has found to cause faulty sugar metabolism [3], although in combination with insulin, it removes glucose from the blood and also plays a key role in fat metabolism [4]. On the other hand, chromium (VI) is lethal to human system because of its mutagenic and carcinogenic properties [5]. Cr(VI), generally occurs in the form of chromate (CrO_4^{2-}) and dichromate ($Cr_2O_7^{2-}$), has the

*Corresponding author.

ability to diffuse through cell [6] and modifies DNA transcription process which can lead to digestive tract and lung cancer [7]. According to the United States Environmental Protection Agency, the maximum contamination level for Cr(VI) in domestic water supplies is 0.05 mg L^{-1} [8], while the permissible limit of Cr(VI) for effluent discharge to inland surface water is 0.1 mg L^{-1}. To comply with these legal requirements and preserve the water quality, removal of toxic chromium from industrial effluents has become almost mandatory. Various techniques are in use for the removal of heavy metals from the industrial discharge, like chemical reduction, solidification, precipitation, lime coagulation and flocculation, ion exchange, membrane separation, etc. but these techniques have serious disadvantages like incomplete removal, sophisticated instrumentation and monitoring, high reagent cost and energy needs, and generation of more toxic waste products [9]. Biosorption is an innovative technology that employs biological materials to accumulate heavy metals from waste water through metabolic process or physicochemical pathways of uptake. Many biosorbents have been used in past years for chromium ion (VI) removal; however, the search for an eco-friendly and low-cost biomaterials remains an active area of research. Biosorption potential of Araucaria leaves [10], Wheat (*Triticum aestivum*) shells [11], *Litchi chinensis* [12], Sunflower head waste-based biosorbent (FSH) [13], *Corinadrum sativum* [14], Wood apple shell [15], *Mangifera indica* bark dust [16], Tobacco leaf [17], Cow dung powder [18], Fruit peel of *Trewia nudiflora* plant [19], and Ornamental plants [20] have recently been tested for Cr(VI) biosorption.

The present study focussed on assessing the ability of environmentally benign adsorbent *Artemisia absinthium*, which belongs to the family Asteraceae. It is herbaceous, perennial plant with fibrous roots originally from Europe and western Asia, presently in parts of Asia, North and South America, within India it is found in the Himalayan region across Jammu and Kashmir in an altitude range of 1,500–2,700 m. It is commonly known as Afsanteen in Arabic and Persian, Vilayathi Afsanteen in Hindi, and Wormwood in English. *A. absinthium* is being a material for research; extracts of the plant have shown to exhibit strong antimicrobial activity, especially against gram-positive pathogenic bacteria [21]. They have also been tested as a potential medication against breast cancer [22]. The chief constituent of *A. absinthium* is a volatile oil. It is usually dark green or sometimes blue in colour, and has a strong odour and bitter taste. The oil contains thujone (absinthol or tenacetone), thujyl alcohol (both free and combined with acetic, isovalerianic, succine, and malic acids), cadinene, phellandrene, and pinene. The herb also contains the bitter glucoside absinthin, absinthic acid, together with tannin, resin, starch, nitrate of potash, and other salts [23]. The material has been selected to explore its adsorption properties towards heavy metals from aqueous solution because of its ease of availability, nontoxic nature, and economic viability.

2. Materials and methods

2.1. Treatment of adsorbent

Seeds of *A. absinthium* were purchased from a Unani medicine shop, Aligarh, UP, India. They were washed thoroughly with double distilled water (DDW) until all impurities adhered on the surface of the seeds were removed. The seeds were then dried in an oven at 60°C. The dried mass was ground and sieved to 150–300 μm. The sieved particles were mixed thoroughly to homogenize the mass. The particles were washed several times with DDW, dried at 60°C, and finally used for all experimental studies.

2.2. Adsorbate solution

Stock solution of Cr(VI) was prepared (1,000 mg L^{-1}) by dissolving required amount of potassium dichromate (AR grade) in DDW and diluted to obtain solutions of required concentration for conducting adsorption experiments. Stock Solutions of Cu(II), Ni(II), and Zn(II) (1,000 mg L^{-1} each) were prepared by dissolving desired quantities of their nitrates in DDW.

2.3. Instrumentation

The scanning electron microscope (SEM, Ametek, USA) was used to record images of the material at different magnifications. Flame atomic absorption spectrometry measurements were made with flame atomic absorption spectrophotometer (AAS, GBC 902 Scientific, Australia) equipped with air/acetylene burner. A pH meter (ELICO-Li, India) was used to measure the pH. A water bath incubator shaker (Narang Scientific Work-CE 0434, India) was used in the isotherm study.

2.4. Adsorption

Adsorption was carried out by batch process. About 0.5 g of adsorbent was placed in a 250 mL conical flask in which 50 mL solution of Cr(VI) of desired concentration was added and the mixture was shaken in temperature-controlled shaker incubator for 24 h. The mixture was then filtered using Whatman filter

paper no. 41 and final concentration of metal ion was determined in the filtrate by AAS. The amount of Cr(VI) adsorbed was calculated by subtracting final concentration from initial concentration.

2.5. Characterization of adsorbent

SEM was used to identify the surface morphology of the adsorbent. Scanning of native and Cr(VI)-adsorbed *A. absinthium* samples was carried out. The images obtained before and after the adsorption of Cr(VI) were compared.

2.6. Effect of temperature

The effect of temperature on the adsorption of Cr(VI) was studied by varying the adsorbent doses from 0.1 to 1.0 g at fixed volume (50 mL) of the Cr(VI) solution with initial concentration of 50 mg L^{-1}. These flasks were kept into temperature-controlled water bath shaker at different temperatures (30–50˚C) for 4 h and then filtered. The final concentration of Cr(VI) in the filtrate from each flask was then determined as described earlier.

2.7. Effect of pH

The effect of pH was investigated in single and multi-metal systems in the pH range of 1–10. The solution of 50 mL Cr(VI) containing 50 mg L^{-1} Cr(VI) was added in a series of conical flasks. The desired pH in each flask was adjusted by adding 0.1 N HCl or 0.1 N NaOH solution. These solutions were then treated with 0.5 g of adsorbent for 24 h in shaker incubator. The solutions were then filtered and final concentrations of Cr(VI) in filtrates were determined as described above. The same procedure was adopted for Cu(II), Ni(II), and Zn(II) solutions. In multi-metal system, 50 mL mixture of Cr(VI), Cu(II), Ni(II), and Zn (II) (50 mg L^{-1} each) was taken in a series of conical flasks and their pHs were adjusted as described above and treated with 0.5 g adsorbent for 24 h. The mixtures were then filtered and metal ions in the filtrate were determined by AAS. To know the effect of ionic strength, Cr(VI) solutions (50 mg L^{-1}) were prepared in 0.1 N KNO_3. The pH of these solutions was adjusted in between 1 and 10 as described above.

2.8. Determination of point of zero charge

Two different doses (0.5 and 0.75 g) of adsorbent were added separately into 0.1 N KNO_3 solutions. Suspension was vigorously agitated for 24 h in temperature-controlled shaker till the pH was invariant; thereafter, a few drops of 1 N KOH were added to the suspension before titration to deprotonate surface sites, and then suspension was titrated with 0.1 N HNO_3 with uninterrupted agitation [24] until neutralization point is reached. Same procedure was repeated with blank solution. The graph was plotted for equilibrium pH values vs. volume of acid added. The point of zero charge (pH_{pzc}) was then calculated at the point of intersection.

2.9. Effect of contact time and initial concentration

Batch adsorption experiments were carried out at different contact times (1, 2, 3, 4, 5, 10, 15, 30, 60, 120, 180, 240, and 300 min) for an initial Cr(VI) concentration in the range of 10–100 mg L^{-1} at pH 2, and the adsorbent dose was 0.5 g in 50 mL solution at 30˚C. Samples were withdrawn from conical flasks after specified time interval and analyzed for residual metal content.

2.10. Breakthrough capacity

About 0.5 g of adsorbent was taken in a glass column (0.6 cm internal diameter) with glass wool support. And 500 mL of Cr(VI) solution with 50 mg L^{-1} initial Cr(VI) concentration (C_o) at pH 2 was passed through the column with flow rate of 1 mL min^{-1}. The effluent was collected initially 10 mL fractions up to 50 mL and remaining solution collected into 50 mL fractions, and the amount of Cr(VI) was determined in each fraction with the help of AAS. The breakthrough curve was plotted for C/C_o vs. volume of the effluent.

2.11. Desorption studies

Desorption studies by column process were also carried out. The exhausted column (from breakthrough capacity experiment) was washed several times with DDW to remove excess of Cr(VI) ions from the column, then 0.01 M NaOH solution was passed through the column with a flow rate 1 mL min^{-1}. The Cr(VI) ions eluted were collected in 10 mL fractions and the amount of Cr(VI) ions desorbed in each fraction was determined by AAS.

3. Results and discussion

3.1. Characterization of adsorbent

SEM images of native and Cr(VI)-treated adsorbent are shown in Fig. 1(a) and (b), which clearly confirmed

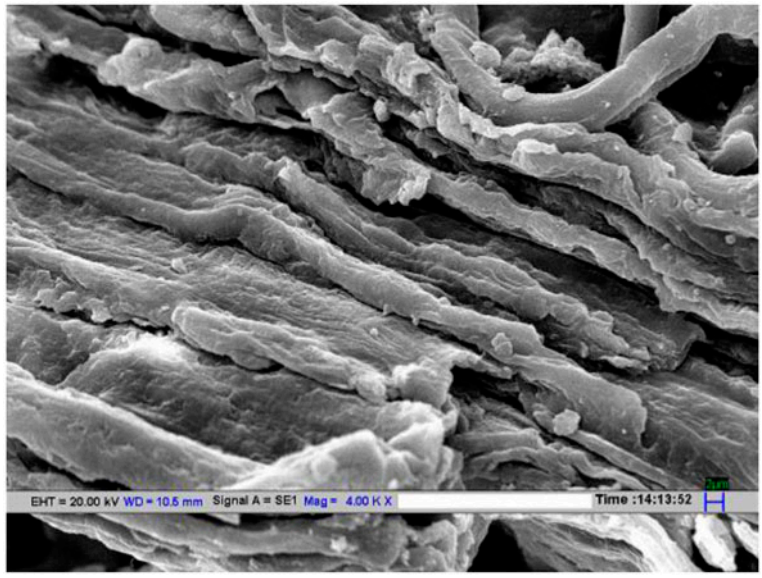

Fig. 1(a). SEM image of *A. absinthium* before adsorption.

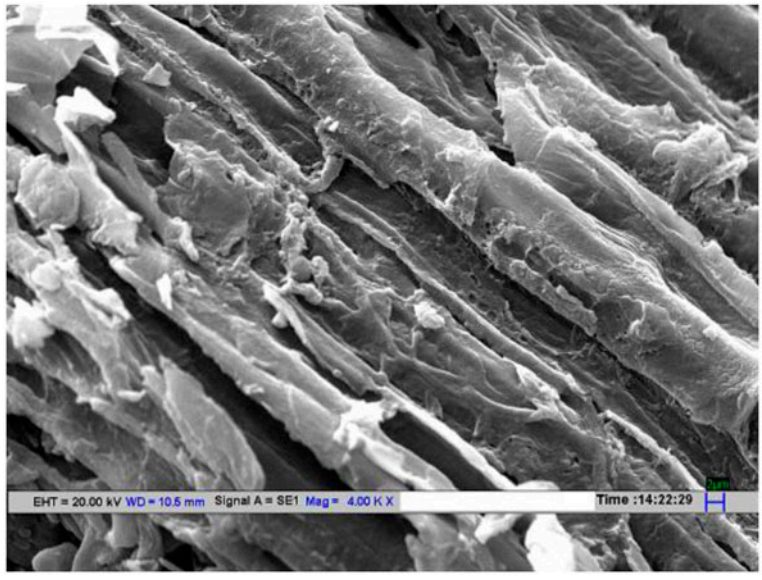

Fig. 1(b). SEM image of *A. absinthium* after Cr(VI) adsorption.

the texture and porous structure of the adsorbent. The surface of the adsorbent was smooth before adsorption and became inhomogeneous and appeared to bulge after adsorption which indicated that the surface has a potential to adsorb the Cr(VI). Moreover, the white patches in the SEM image of treated adsorbent might be due to the adsorption of Cr(VI) on the surface of the *A. absinthium* seeds.

3.2. Effect of contact time and initial Cr(VI) concentration

The mechanism of the metal uptake generally depends on the initial concentration of heavy metals in contact with the adsorbent. At low concentration, the specific sites are responsible for the adsorption, while on increasing metal concentrations, the specific sites are saturated and the adsorption sites are filled [25]. Adsorption studies at pH 2 were carried

out at different intervals of time (Fig. 2). The equilibrium time for the adsorption of Cr(VI) increased initially with increasing concentration and became independent at concentration above 80 mg L^{-1}. The equilibrium time was found to be 15, 30, 60, and 120 min at 10, 20, 50, and 60 mg L^{-1} and 180 min for both 80 and 100 mg L^{-1} concentrations, respectively. The adsorption capacity increased with increase in initial concentration because of the increase in concentration gradient and driving force with increase in concentration. The adsorption capacity of Cr(VI) at equilibrium was found to be 0.39, 1.12, 2.6, 3.3, 4.4, and 4.5 mg g^{-1}, respectively, at initial concentration 10, 20, 50, 60, 80, and 100 mg L^{-1}.

3.3. Effect of pH

The adsorption of Cr(VI), Cu(II), Ni(II), and Zn(II) in single-metal system and multi-metal system was carried out over a pH ranges 2–10. The state of metal ions in solution strongly depends on the pH. The acidity and basicity of the solutions can influence the properties of the adsorbent surface and speciation of metal ions. This is partly due to the fact that the hydrogen ion itself is a strong competing adsorbate, and partly due to the chemical speciation of metal ions under the influence of the solution pH. At acidic condition (pH 2–6), the predominant species of Cr(VI) are $Cr_2O_7^{2-}$ and $HCrO_4^-$ [26]; therefore, it can be inferred that Cr(VI) adsorbed at pH 2 mainly in the form of $HCrO_4^-$ ions but below pH 2, adsorption decreased again (28.8% at pH 1) due to the formation of unionized H_2CrO_4. The adsorption of metal ions depends upon both the nature of the adsorbent surface and the species distribution of the metal ions in the aqueous solution. In the case of Cr(VI) adsorption, experiments were carried out by varying pH from 1 to 10. The results in Fig. 3(a) indicated that Cr(VI) adsorption was considerably affected by the pH. Adsorption increased from 13.4 to 96% when pH decreased from 8 to 2. The increase in Cr(VI) adsorption with decrease in solution pH was also observed on peat [27], fungal biomass [28], bacterium biomass [29], banana pith [30], rice straw [31], and green alga [32]. The maximum adsorption of Cr(VI) observed at pH 2 (96%) was mainly due to the ionic interaction between the positively charged surface of the adsorbent and negatively charged Cr(VI) ions, and there was not a remarkable change in the final pH ($pH_f = 2.7$) indicating that the surface of the adsorbent was protonated to a higher extent which leads to strong attraction between these oxy-anions of Cr(VI) and the positively charged surface of the adsorbent. At the higher pH (6–10), the predominant species are then CrO_4^{2-} and $Cr_2O_7^{2-}$ and there was a dual competition of both anions (CrO_4^{2-} and $Cr_2O_7^{2-}$) with OH^-, which resulted a decrease in Cr(VI) adsorption. Adsorption of Cr(VI) at different pH in presence of KNO_3 (to maintain ionic strength) indicated that the presence of electrolyte decreased the Cr(VI) adsorption at pH 2 as shown in Fig. 3(b) This could be attributed to the competition between nitrate and chromate anions on the active site of the adsorbent. The pH_{pzc} of *A. absinthium* in DDW was found to be 3.9 (Fig. 3(b)) showing that surface was positively charged below pH 3.9, neutral at pH 3.9, and negatively charged above pH 3.9, and hence adsorption of Cr(VI) was maximum below pH_{pzc} due to electrostatic attraction between positively charged adsorbent surface and negatively charged Cr(VI) ions.

In case of single-metal system, the influence of pH on the adsorption of Cu(II) was examined at different pH ranging from 1 to 10 (Fig. 3(c)). The Cu(II) adsorption increased significantly from 0 to 93% at

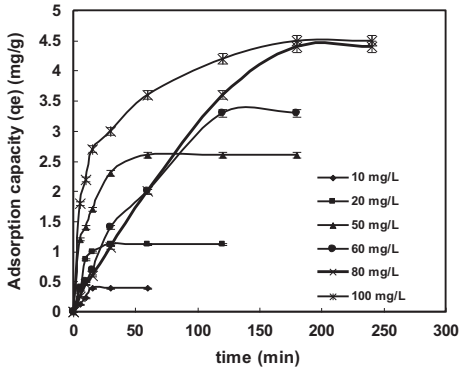

Fig. 2. Effect of time and initial concentrations on the adsorption of Cr(VI) at pH 2.

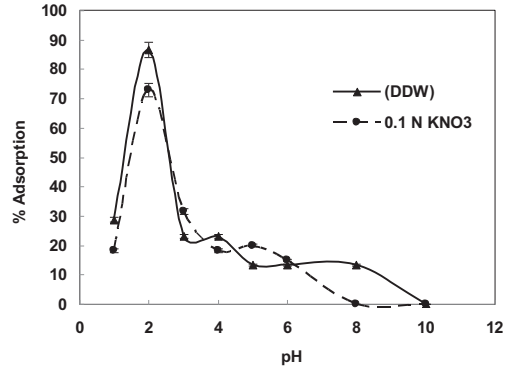

Fig. 3(a). Effect of pH on the adsorption of Cr(VI).

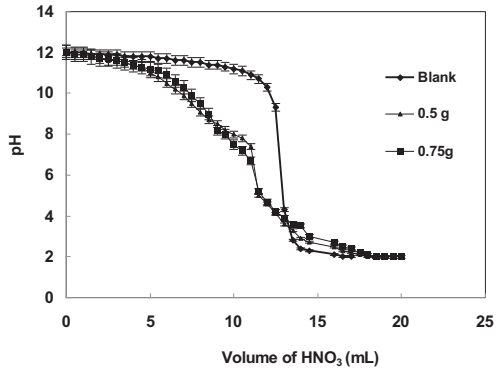

Fig. 3(b). Point of zero charge.

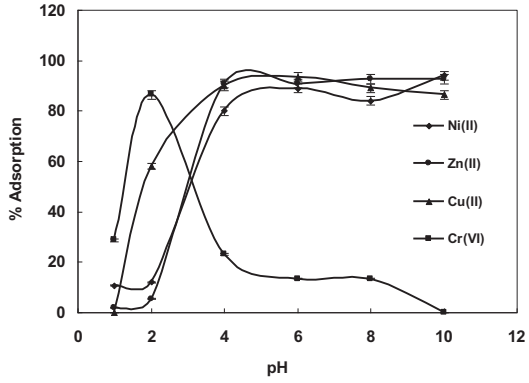

Fig. 3(c). Adsorption of Cr(VI),Cu(II), Ni(II) and Zn(II) at different pH (single-metal system).

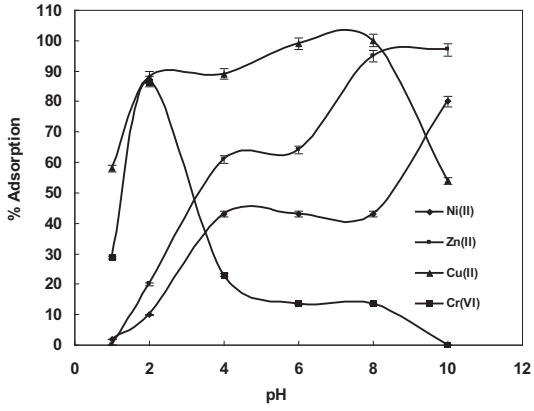

Fig. 3(d). Adsorption of Cr(VI), Cu(II), Ni(II) and Zn(II) at different pH (multi-metal system).

pH ranging from 1 to 6. The adsorption of Cu (II) was least at pH 1 and increased rapidly up to pH 4 due to the deprotonation of the adsorption sites. Over the range $4 < pH < 5$, Cu(II) ions were adsorbed both as Cu^{2+} and $Cu(OH^{+})$ ions since both the species exist over this pH range [33]. At pH 1–3, copper exists as Cu^{2+}; in the range of pH 3–5, two species i.e. Cu^{2+} and $Cu(OH)^{+}$ are found; and at pH 6, Cu^{2+} exists as $Cu(OH)^{+}$ and $Cu(OH)_2$. It was observed from Fig. 3(c) that as pH increased, adsorption percentage of Cu(II) also increased and reached maximum value at pH 6, then slightly decreased as pH increased further up to pH 10 indicating that maximum adsorption percentage of Cu(II) occurred at pH 6 and at $pH > 6$, Cu(II) formed $Cu(OH)_2$ in a large quantities; therefore, at higher pH (>pH 6), Cu(II) ions were precipitated in the form of $Cu(OH)_2$ and caused micro-precipitation.

It has been observed that under highly acidic conditions (pH 1–2), the percent adsorption of Ni(II) was constant with least value, while the adsorption increased as pH increased and reached maximum at pH 4 because at $pH \leq 6$, Ni(II) existed as Ni^{2+} (Fig. 3(c)). The low removal efficiency at low pH was apparently due to the presence of higher concentration of H^{+} in the solution which compete Ni(II) ions for the adsorption sites of the *A. absinthium*. It was clear that with increase in pH, the H^{+} concentration decreased leading to increased adsorption of Ni(II) up to pH 4, as with increasing pH further, the % adsorption also increased. At $pH > 6$, the nickel ions get precipitated because at $pH \geq 6$, $Ni(OH)_2$ is the dominant species. The adsorption of Zn(II) ions at various pH values may be explained in a similar manner. The adsorption of Zn(II) was zero at pH 1 and negligible at pH 2 (Fig. 3(c)) but when pH of the solution increased, the adsorption of Zn(II) increased and reached to maximum value at pH 6 and then remained constant up to pH 10. In multi-metal system, the optimum pH for the adsorption of Cu(II) and Zn(II) was found to be 6, Ni(II) at pH 4, and Cr(VI) at pH 2 (Fig. 3(d)). It is important to note that adsorption of Cr(VI) was not affected in presence of Cu(II), Ni(II), and Zn(II) ions indicating that adsorption of Cr(VI) is specific on *A. absinthium* seeds.

3.4. Adsorption isotherms

In order to optimize the design of adsorption system for the removal of Cr(VI) from aqueous solution, it is important to explain the relationship between adsorbed metal ion per unit weight of adsorbent (q_e) and residual concentration of metal ion in solution (C_e) at equilibrium. The analysis of the adsorption isotherm data by fitting them to different adsorption isotherm models is an important step to find the suitable adsorption isotherm model that can be used for design purposes. Experimental data were fitted in the Langmuir, Freundlich, Temkin, Halsey, and Dubinin–Redushkeuich (D–R) models at different temperatures. The fitting procedure was performed by using R

software version 2.10.1 (14 December 2009). In order to evaluate the fitness of the data, determination coefficient (R^2), error analysis, and chi-square test (χ^2) were evaluated between experimental and calculated data from each model.

According to Langmuir model [34], the adsorption occurs on a homogenous surface forming monolayer of adsorbate with constant heat of adsorption for all sites without interaction between adsorbed molecules [35]. The linear form of Langmuir model may be given as follows:

$$\frac{1}{q_e} = \frac{1}{q_m} \times \frac{1}{b} \times \frac{1}{C_e} + \frac{1}{q_m} \tag{1}$$

where C_e is the equilibrium concentration of Cr(VI) in the solution ($mg\,L^{-1}$), q_e is the amount of Cr(VI) adsorbed per unit weight of adsorbent ($mg\,g^{-1}$), q_m is the amount of Cr(VI) required to form monolayer ($mg\,g^{-1}$), and b is a constant related to energy of adsorption ($L\,mg^{-1}$) which represents enthalpy of adsorption and should vary with temperature. The values of b and q_m were calculated from the slope and intercept of the linear plots of $1/q_e$ vs. $1/C_e$ at different temperatures. The Langmuir parameters are reported in Table 1. The isotherm was found to be linear at 30, 40, and 50°C, showing that data were correctly fitted in a Langmuir relation. The monolayer saturation capacity (q_m) was found to be 46.99, 14.21, and 10.59 $mg\,g^{-1}$ at 30, 40, and 50°C respectively. The fitting of data in Langmuir isotherm confirmed the monolayer coverage of Cr(VI) and also the homogeneous distribution of active sites on the adsorbent.

The Freundlich model [36] is an empirical equation based on the adsorption of adsorbate onto heterogeneous surface. The linear form of Freundlich model can be represented as follows:

$$\log q_e = \log K_f + \frac{1}{n} \log C_e \tag{2}$$

where C_e is the equilibrium concentration in $mg\,L^{-1}$ and q_e is the amount of Cr(VI) adsorbed per unit weight of adsorbent ($mg\,g^{-1}$). K_f is the Freundlich constant which indicates the relative adsorption capacity of the adsorbent related to bonding energy and n is the heterogeneity factor representing the deviation from linearity of adsorption and is also known as Freundlich coefficient. As n approaches zero, the surface site heterogeneity increases. In the present study, the value of $n > 1$ (Table 1) at all temperatures indicated favorable adsorption at Cr(VI) [37]. A plot of $\log q_e$ vs. $\log C_e$ generated straight line and values of $1/n$ and K_f can be calculated from the slope and intercept. The data obtained from this model indicated that the values of K_f and n increased with the increase in temperature from 30 to 50°C.

Temkin isotherm [38] describes the effect of indirect adsorbate–adsorbent interaction and assumes that the decrease in the heat of adsorption is linear rather than logarithmic as implied in Freundlich isotherm. The linearized form of Temkin equation can be represented as follows:

$$q_e = \left(\frac{RT}{b}\right) \times \ln A + \left(\frac{RT}{b}\right) \times \ln C_e \tag{3}$$

where $(RT/b) = B_T$, R is universal gas constant, T is absolute temperature, and b is Temkin isotherm constant. A_T ($g\,L^{-1}$) and B_T ($J\,mol^{-1}$) are Temkin constants related to adsorption potential and heat of adsorption. The values of A_T and B_T were calculated from the slope and intercept of the plot of q_e vs. ln C_e (data are shown in Table 1). The best linear fitting with higher correlation coefficients at higher temperatures indicated that there was strong interaction between the adsorbate and adsorbent.

The Halsey isotherm model is suitable for multilayer adsorption. The linearized form of Halsey isotherm is commonly represented by the relation.

$$\ln q_e = \left[\frac{1}{n} \ln K_h\right] - \frac{1}{n} \ln C_e \tag{4}$$

where K_h and n are the Halsey isotherm constants and exponent, respectively. The Halsey isotherm parameters are presented in Table 1. The best fitting of the Halsey isotherm equation was at 30°C indicated the heteroporosity (i.e. macrospore and microspore) of the *A. absinthium* [39].

D–R isotherm [40] does not assume a homogenous surface or a constant sorption potential [41]. It is commonly represented as:

$$\ln q_e = \ln q_m - \beta \varepsilon^2 \tag{5}$$

where β is the activity coefficient constant ($mol^{-2}\,J^{-2}$), q_m is the maximum adsorption capacity ($mol\,g^{-1}$), q_e is the equilibrium adsorption capacity ($mol\,g^{-1}$), and ε^2 is the Polanyi potential. The value of ε can be calculated from the relation.

$$\varepsilon = RT \ln \left(1 + \frac{1}{Ce}\right) \tag{6}$$

Table 1
Adsorption isotherm parameters for the adsorption of Cr(VI) on *A. absinthium*

Isotherms	Parameters	30℃	40℃	50℃
Langmuir	b (L mg^{-1})	0.010	0.190	10.590
	q_m (mg g^{-1})	46.990	14.210	23.364
	R^2	0.991	0.999	0.996
	RSE	0.015	0.001	0.008
	p-value	<0.05	<0.05	<0.05
Freundlich	K_f (mg g^{-1}) (L mg^{-1})$^{1/n}$	0.606	2.440	3.400
	n (g L^{-1})	1.100	1.700	2.180
	R^2	0.999	0.979	0.976
	χ^2	0.054	0.000	0.120
	RSE	0.005	0.061	0.046
	p-value	<0.05	<0.05	<0.05
Temkin	A_T (L mg^{-1})	0.349	1.960	4.167
	B_T (J mol^{-1})	4.280	3.061	2.495
	R^2	0.934	0.998	0.996
	χ^2	0.259	0.009	0.024
	RSE	0.005	0.218	0.211
	p-value	<0.05	<0.05	<0.05
Dubinin–Redushkeuich	q_m (mol g^{-1})	0.004	0.001	0.001
	$\beta \times 10^{-9}$	8.310	4.425	3.457
	E (kJ mol^{-1})	7.760	10.850	12.003
	R^2	0.986	0.988	0.988
	$\chi^2 \times 10^{-9}$	1.326	0.195	0.234
	RSE	0.076	0.069	0.076
	p-value	<0.05	<0.05	<0.05
Halsey	n_h	−1.085	1.700	2.180
	K_h	0.561	4.600	14.400
	RSE	0.800	0.218	0.211
	R^2	0.990	0.979	0.976
	χ^2	0.041	0.117	0.120
	p-value	<0.05	<0.05	<0.05

where T is the temperature in Kelvin and R is gas constant (J mol^{-1} K^{-1}). Hence, by plotting ln q_e vs. ε^2, the value of q_m from the intercept and β from the slope can be calculated. The results are reported in Table 1. The constant β gives an idea about the mean free energy (E) (kJ mol^{-1}) of adsorption of the molecule of adsorbate when it is transferred to the surface of the solid from infinity and can be calculated using the following relation [40]:

$$E = \frac{1}{\sqrt{(-2\beta)}} \tag{7}$$

The values of E lie between 8 and 16 kJ mol^{-1} and depicts chemisorptions and if $E < 8$ kJ mol^{-1}, the adsorption process is of physical in nature [42]. The high value of mean free energy ($E = 10$–12 KJ mol^{-1}) of adsorption indicated that the adsorption process is chemical in nature and most probably proceeded via ion exchange (Table 1). On comparing the linear regression values, it can be concluded that the Langmuir and D−R isotherms were capable of representing the data more satisfactorily ($R^2 = 0.9917 - 0.9885$) indicating the applicability of these isotherms. The increase in the value of binding energy (b L mg^{-1}) with temperature indicated that adsorption was favorable at higher temperature. Temkin model also indicated that the value of A_T increased with increase in temperature showing that adsorption process was favorable at high temperature. Freundlich isotherm indicated an increase in K_f with increasing temperature supporting

that adsorption was favorable at higher temperature. Halsey model was best fitted at 30°C ($R^2 = 0.9997 - 0.9904$) indicating heteroporous nature of the adsorbent. The maximum monolayer adsorption capacity (q_m) of *A. absinthium* was compared with other adsorbents reported in the literature (Table 2) and it was found that *A. absinthium* represented maximum adsorption capacity towards Cr(VI) ions [43–49].

3.5. Thermodynamic

The effect of temperature on the adsorption of Cr(VI) was studied at temperature ranging from 30 to 50°C. Thermodynamic parameters such as standard free energy change (ΔG^0), standard enthalpy change (ΔH^0), and standard entropy change (ΔS^0) were calculated using the following relations [50]. K_c can be calculated by Eq. (8).

$$K_c = \frac{C_{Ad}}{C_e} \tag{8}$$

where K_c is the distribution constant, and C_{Ad} and C_e are equilibrium concentrations of Cr(VI) on the adsorbent and in the solution, respectively.

The Gibbs energy change (ΔG^0) indicates the degree of spontaneity of an adsorption process, and a higher negative value reflects a more energetically favorable adsorption. According to thermodynamic law, ΔG^0 of adsorption was calculated from the following equation:

$$\Delta G^0 = -RT \ln K_c \tag{9}$$

where K_c is the thermodynamic equilibrium constant without units, T is the absolute temperature in Kelvin, and R is the gas constant. The values of ΔH^0 and ΔS^0 were calculated from the following Van't Hoff equation.

$$\ln K_c = -\frac{\Delta H^0}{RT} + \frac{\Delta S^0}{R} \tag{10}$$

A plot of $\ln K_c$ vs. $1/T$ gave straight line, and ΔH^0 and ΔS^0 were calculated from the slope and intercept (Fig. not shown). These thermodynamic parameters estimates can offer insight into the type and mechanism of an adsorption process (Reported in Table 3). The negative values of ΔG^0 indicated spontaneous nature of the process and more negative values with increased in temperature showed that an increase in temperature favored the adsorption process. Positive values of ΔH^0 indicated endothermic nature of the adsorption, whereas the positive value of ΔS^0 indicated the increased randomness at the solid/solution interface during the adsorption of Cr(VI).

3.6. Adsorption kinetics

In order to understand the kinetics of removal of Cr(VI), various kinetic models were tested with the experimental data. Probably, the earliest known and one of the most widely used kinetic equations for the adsorption of a solute from a liquid solution is Lagergren's Equation or the pseudo-first-order equation [51].

The linear form of pseudo-first-order kinetics equation is given as follows:

$$\log (q_e - q_t) = -\left(\frac{K_1}{2.323}\right) \times t + \log\ q_e \tag{11}$$

where q_e is the amount of Cr(VI) adsorbed per unit weight of adsorbent at equilibrium or adsorption

Table 2
Comparison of adsorption capacity of Cr(VI) with other adsorbents

Name of adsorbent	Maximum adsorption capacity q_m (mg g^{-1})	References
Almond	10.00	[43]
Cactus	7.08	[43]
Pine needle	21.50	[43]
Walnut shell	1.33	[44]
Helianthus annuus	7.20	[45]
Olive pomace	4.00	[46]
Sawdust	41.50	[47]
Wheat bran	40.80	[48]
Pleurotus ostreatus	10.75	[49]
Artimisia absinthium	46.90	Present study

Table 3
Thermodynamics parameters for the adsorption of Cr(VI) at pH 2

Temperature (°C)	K_c	ΔG^0 (kJ mol^{-1})	ΔH^0 (kJ mol^{-1})	ΔS^0 (kJ mol^{-1} K^{-1}
30	10.34	−05.89		
40	44.25	−09.86	82.41	00.29
50	82.27	−11.84		

capacity (mg g^{-1}), q_t is the amount of Cr(VI) adsorbed per unit weight of adsorbent at any given time t, and K_1 is the rate constant for pseudo-first-order model. The values of K_1 and q_e were calculated from slope and intercept of the linear plot of log $(q_e - q_t)$ vs. t at various concentrations. A plot of log $(q_e - q_t)$ vs. t gave straight lines confirming the applicability of the pseudo-first-order rate equation (Fig. not shown). The parameters of pseudo-first-order model are summarized in Table 4. The values of determination of coefficient were in the range 0.9528–0.9910. The coefficient of determination value was reasonably high but the calculated adsorption capacity ($q_{e(cal)}$) obtained from the model did not give reasonable values when compared with experimental adsorption capacity ($q_{e(exp)}$). This finding suggested that the adsorption process did not follow the pseudo-first-order adsorption rate expression.

The pseudo-second-order rate expression is used to describe chemisorption involving valance forces through the sharing or exchange of electrons between the adsorbent and adsorbate as covalent forces, and ion exchange [52]. The pseudo-second-order kinetic rate equation is given as follows:

$$\frac{t}{q_t} = \frac{1}{K_2 \times q_e^2} + \frac{1}{q_e} \times t \tag{12}$$

where K_2 is the rate constant of pseudo-second-order adsorption (g mg^{-1} min^{-1}). Plots of t/q_t vs. t for all experimental concentrations gave straight lines (Fig. not shown) indicating the applicability of pseudo-second-order adsorption kinetic model, and values of q_e and K_2 were calculated from the slope and intercept, respectively. The initial adsorption rate, h (mg g^{-1} min^{-1}), is expressed [53] as follows:

$$h = K_2 \times q_e^2 \tag{13}$$

The parameters of the pseudo-second-order adsorption kinetic model are tabulated in Table 5. The determination coefficient values of the pseudo-second-order model exceeded 0.99 and the $q_{e(cal)}$ values were more consistent with the experimental values of adsorption capacity $q_{e(exp)}$. Therefore, the pseudo-second-order model better represented the adsorption kinetics.

Elovich equation [54] is a rate equation based on the adsorption capacity commonly expressed as follows:

$$\frac{dq_t}{d_t} = \alpha \exp\left(-\beta q_t\right) \times t^{1/2} + I \tag{14}$$

where α (mg g^{-1} min^{-1}) is the initial adsorption rate and β (g mg^{-1}) is desorption constant related to the extent of the surface coverage activation energy for chemisorption. Eq. (19) is simplified by assuming $\alpha\beta >> t$ and by applying the boundary conditions $q_t = 0$ at $t = 0$ and $q_t = q_t$ at $t = t$ as given by equation as follows: (Eq. (15))

$$q_t = \frac{1}{\beta}\ln\left(\alpha\beta\right) + \frac{1}{\beta}\ln t \tag{15}$$

Table 4
Pseudo-first-order kinetic parameters for sorption of Cr(VI) at pH 2

Concentration (C_o) (mg L^{-1})	$q_{e(exp)}$ (mg g^{-1})	$q_{e(cal)}$ (mg g^{-1})	K_1	R^2
10	0.96	0.69	0.0069	0.980
20	1.86	1.04	0.0046	0.952
50	4.50	2.96	0.0046	0.976
60	5.10	4.63	0.0046	0.991
80	5.60	3.17	0.0046	0.929
100	6.67	7.17	0.0069	0.974

Table 5
Pseudo-second-order kinetic parameters for sorption of Cr(VI) at pH 2

Concentration (C_o) (mg L^{-1})	$q_{e(exp)}$ (mg g^{-1})	$q_{e(cal)}$ (mg g^{-1})	h (mg g^{-1} min^{-1})	K_2 (g mg^{-1} min^{-1})	R^2
10	0.96	1.03	0.02	0.025	0.998
20	1.86	1.91	0.07	0.019	0.994
50	4.50	4.76	0.12	0.005	0.990
60	5.10	6.02	0.05	0.001	0.991
80	5.60	5.59	0.19	0.006	0.990
100	6.67	9.80	0.04	0.000	0.991

The slope and intercept of the linear plot of q_t vs. ln t resulted in the estimation of kinetic constants α and β. The coefficients of determination (R^2) were obtained in the range of 0.944 to 0.986 for all Cr(VI) concentrations (10−100 mg L^{-1}) and indicated that it could not adequately describe Cr(VI) adsorption kinetics (Data not shown).

The kinetic data were analyzed using intra-particle diffusion model [55] to elucidate the diffusion mechanism. It is commonly represented as follows:

$$q_t = K_{id} \times t^{1/2} + I \quad (16)$$

where K_{id} (mg g^{-1} min^{-1}) is the intra-particle diffusion rate constant, I (mg g^{-1}) is another constant that gives idea about the thickness of a boundary layer, and q_t is the amount of Cr(VI) absorbed (mg g^{-1}) at time t (min). Plots of q_t vs. $t^{1/2}$ are shown in Fig. 4 at various initial Cr(VI) concentrations. In the present work, the plot presented multi-linearity indicating that three steps were involved. The first, sharper portion represented external surface adsorption or faster adsorption stage. The second portion described a gradual adsorption stage involving intra-particle diffusion. The third portion was attributed to the final equilibrium stage, where intra-particle diffusion started to slow down due to the extremely low adsorbate concentrations in the solution [56]. The slope of the plot was defined as the intra-particle diffusion parameter K_{id} (mg g^{-1} $min^{-1/2}$) [57]. On the other hand, the intercept of the plot reflected the boundary layer effect. The larger the intercept, the greater will be the contribution of the surface adsorption in the rate-limiting step (Table 6). This indicated that intra-particle diffusion was involved in the Cr(VI) adsorption, but it was not the rate-controlling step. The sensitivity analyses of all the four kinetic models were carried out. The change in amount adsorbed on the surface of adsorbent with the change in same time interval was less for second-order kinetic model as compared to other two models. This indicated that the second-order rate kinetic model was less sensitive as compared to pseudo-first-order and intra-particle diffusion kinetic models.

3.7. Breakthrough capacity

Breakthrough curve is the most effective column process making the optimum use of the concentration gradient between the solute adsorbed by the adsorbent and that remaining in the solution. The column is operational until the metal ions in the effluent start appearing and for practical purposes, the working life of the column is over called breakthrough point. This is important in process design because it directly affects the feasibility and economics of the process [58]. Breakthrough curve (Fig. 5) showed that 350 mL Cr(VI) solution with a concentration of 50 mg L^{-1} could be passed through the column packed with 0.5 g adsorbent at pH 2 without detecting Cr(VI) in the effluent. The breakthrough and exhaustive capacities were found to be 35 and 45 mg g^{-1}, respectively.

3.8. Desorption

In order to explore the economic viability of the adsorbent, the desorption of Cr(VI) after adsorption was carried out by column process. The adsorption of

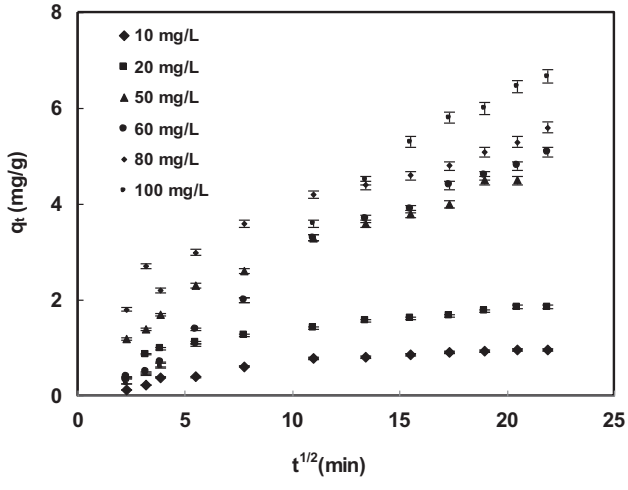

Fig. 4. Intra-particle diffusion plots for the adsorption of Cr(VI).

Table 6
Intra-particle diffusion parameters for the adsorption of Cr(VI) at pH 2

Concentration ($mg\,L^{-1}$)	K_{id1} ($mg\,g^{-1}\,min^{-1/2}$)	K_{id2} ($mg\,g^{-1}\,min^{-1/2}$)	K_{id3} ($mg\,g^{-1}\,min^{-1/2}$)	I_1 ($mg\,g^{-1}$)	I_2 ($mg\,g^{-1}$)	I_3 ($mg\,g^{-1}$)	R_1^2	R_2^2	R_3^2
10	0.163	0.070	0.017	−0.258	0.039	0.586	0.967	0.971	0.946
20	0.394	0.050	0.043	−0.479	0.861	0.932	0.929	0.987	0.904
50	0.349	0.178	0.156	0.362	0.256	1.366	0.987	0.976	0.899
60	0.311	0.133	0.126	−0.400	1.864	2.213	0.979	0.980	0.999
80	0.245	0.216	0.085	1.250	1.852	3.310	1.000	0.990	0.992
100	0.214	0.464	0.248	−0.230	−1.516	1.337	0.999	0.997	0.973

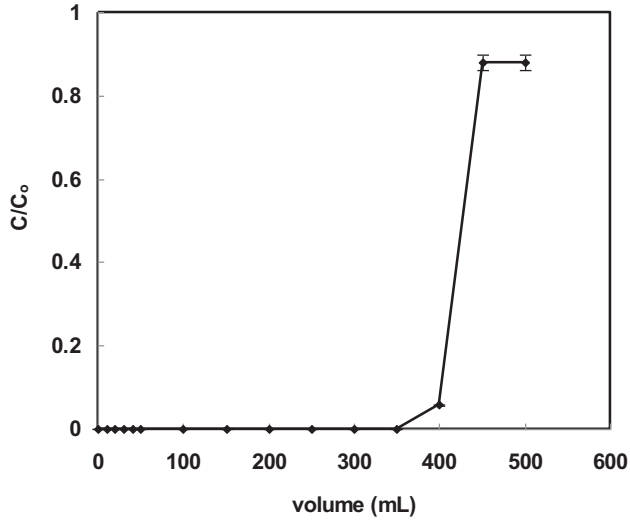

Fig. 5. Breakthrough capacity of Cr(VI) at pH 2.

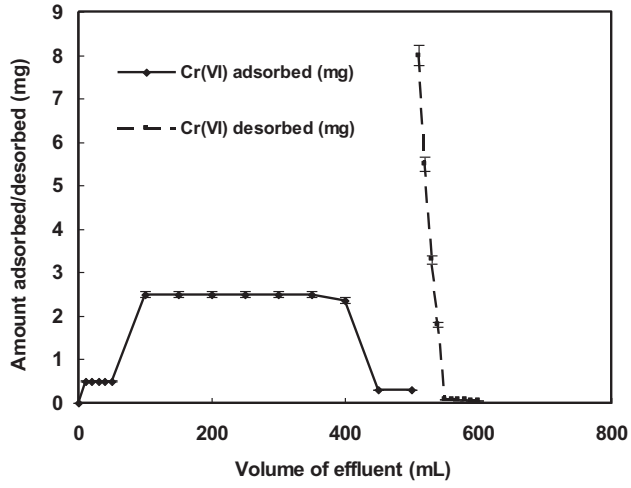

Fig. 6. Adsorption/desorption of Cr(VI) by column process.

Cr(VI) with $50\,mg\,L^{-1}$ initial concentration was 90.9% at pH 2 and 93.05% Cr(VI) was desorbed by using 0.01 N NaOH as desorbing solution (Fig. 6). This may be ascribing to the fast mass transfer rate between the surface of the adsorbent and the desorbing agent. The maximum desorption demonstrated high reusability of the adsorbent, making removal and recovery of Cr(VI) from wastewater containing Cr(VI) a more sustainable and economical alternative.

4. Conclusions

A. absinthium seeds have shown remarkable adsorption capacity towards Cr(VI), Cu(II), Ni(II), and Zn(II) ions. The adsorption of Cr(VI) was

maximum at pH 2, while Cu(II) and Zn(II) at pH 6 and Ni(II) at pH 4 were adsorbed appreciably. The adsorption of Cr(VI) was fast and maximum amount of Cr(VI) could be adsorbed within 60 min at 60 mg L^{-1} initial Cr(VI) concentration. In multi-metal system, it was found that adsorption of Cr(VI) was not affected in the presence of Cu(II), Ni(II), and Zn(II) at pH 2. Langmuir, Freundlich, and Temkin isotherms indicated that adsorption of Cr(VI) was favorable at higher temperatures. Kinetic data showed the better applicability of pseudo-second-order model confirming that adsorption of Cr(VI) was chemisorption in nature. Column experiments showed that the breakthrough begins at 350 mL. Desorption study showed that maximum amount of Cr(VI) (93.05%) could be recovered using 0.01 N NaOH solution as adsorbing agent by column process. It may be concluded that seeds of *A. absinthium* may be utilized for the removal and recovery of Cr(VI) from aqueous solution containing Cu(II), Ni(II), and Zn(II) ions.

Acknowledgments

Authors thank the Chairman (Prof. Ali Mohammad), Department of Applied chemistry, Z. H. College of Engineering and Technology, Aligarh Muslim University, Aligarh (India), for providing research facilities.

References

[1] L. Friberg, C.G. Elinder, Encyclopaedia of Occupational Health, 3rd ed., International Labour Organization, Geneva, 1985.
[2] S.A. Katz, The analytical biochemistry of chromium, Environ. Health Perspect. 92 (1991) 13–16.
[3] M.D. Walter Mertz, Effects and metabolism of glucose tolerance factor, Nutr. Rev. 33 (1975) 129–135.
[4] D.G. Barceloux, Chromium, J. Toxicol. Clin. Toxicol. 37 (1999) 173–194.
[5] C.R.K. Murti, P. Viswanathan, Toxic Metal in the Indian Environment, Tata McGraw-Hill. New Delhi, 1991.
[6] M.S. Hosseini, A.R.R. Sarab, Cr(III)/Cr(VI) speciation in water samples by extractive separation using Amberlite CG-50 and final determination by FAAS, Int. J. Environ. Anal. Chem. 87 (2007) 375–385.
[7] DC. US Department of Health and Human Services, Toxicological Profile for Chromium, Public Health Services Agency for Toxic substances and Diseases Registry, Washington, DC, 1991.
[8] USEPA, USEPA Drinking Water Regulations and Health Advisories, EPA 822-B 96-002, USEPA, Washington, DC), 1996.
[9] Z. Aksu, F. Gonen, Z. Demircan, Biosorption of chromium(VI) ions by Mowital B_3OH resin immobilized activated sludge in a packed bed: Comparison with granular activated carbon, Process. Biochem. 38 (2007) 175–186.
[10] D. Shukla, P.S. Vankar, Efficient biosorption of chromium(VI) ion by dry Araucaria leaves, Environ. Sci. Pollut. Res. 19 (2012) 2321–2328.
[11] P.D. Saha, A. Dey, P. Marik, Batch removal of chromium (VI) from aqueous solutions using wheat shell as adsorbent: Process optimization using response surface methodology, Desalin. Water Treat. 39 (2012) 95–102.
[12] R.A.K. Rao, F. Rehman, M. Kashifuddin, Removal of Cr(VI) from electroplating wastewater using fruit peel of leechi (*Litchi chinensis*), Desalin. Water Treat. 49 (2012) 136–146.
[13] M. Jain, V.K. Garg, K. Kadirvelu, Chromium removal from aqueous system and industrial wastewater by agricultural wastes, Biorem. J. 17 (2013) 30–39.
[14] R.A.K. Rao, M. Kashifuddin, Adsorption properties of coriander seed powder (*Coriandrum sativum*): Extraction and pre-concentration of Pb(II), Cu(II) and Zn(II) ions from aqueous solution, Adsorpt. Sci. Technol. 30 (2012) 127–146.
[15] K.M. Doke, M. Yusufi, R.D. Joseph, E.M. Khan, Biosorption of hexavalent chromium onto wood apple shell: Equilibrium, kinetic and thermodynamic studies, Desalin. Water Treat. 50 (2012) 170–179.
[16] A. Manjusha, N. Gandhi, D. Sirisha, Adsorption of chromium (VI) from aqueous solution by using *Mangifera indica* bark dust, Universal J. Environ. Res. Technol. 2 (2012) 108–111.
[17] Y. Chen, G. Tang, Q.J. Yu, T. Zhang, Y. Chen, T. Gu, Biosorption properties of hexavalent chromium on to biomass of tobacco-leaf residues, Environ. Technol. 30 (2009) 1003–1010.
[18] N.S. Barot, H.K. Bagla, Eco-friendly waste water treatment by cow dung powder (adsorption studies of Cr(III), Cr(VI) and Cd(II) using tracer technique), Desalin. Water Treat. 38 (2012) 104–113.
[19] P. Bhattacharya, P. Banerjee, K. Mallick, S. Ghosh, S. Majumdar, A. Mukhopadhyay, S. Bandyopadhyay, Potential of biosorbent developed from fruit peel of *Trewia nudiflora* for removal of hexavalent chromium from synthetic and industrial effluent: Analyzing phytotoxicity in germinating Vigna seeds, J. Environ. Sci. Health. Part A Toxic/Hazard. Subst. Environ. Eng. 48 (2013) 706–719.
[20] Q. Miao, J. Yan, Comparison of three ornamental plants for phytoextraction potential of chromium removal from tannery sludge, J. Mater. Cycles Waste Manage. 15 (2013) 98–105.
[21] Y.C. Fiamegos, P.L. Kastritis, V. Exarchou, H. Han, A.M.J.J. Bonvin, Antimicrobial and efflux pump inhibitory activity of caffeoylquinic acids from *Artemisia absinthium* against gram-positive pathogenic bacteria, PLoS ONE 6 (2011) e18127.
[22] G. Shafi, T.N. Hasan, N.A. Syed, A.A. Al-Hazzani, A.A. Alshatwi, A. Jyothi, A. Munshi, *Artemisia absinthium* (AA): A novel potential complementary and alternative medicine for breast cancer, Mol. Biol. Rep. 39 (2012) 7373–7379.
[23] M. Grieve, A. Modern Herbal, ISBN: 0486227987, 0486227995, 1/2 (1931) 1–919.
[24] K. Bourikas, J. Vakros, C. Kordulis, A. Lycourghiotis, Potentiometric mass titrations: Experimental and

theoretical establishment of a new technique for determining the point of zero charge (PZC) of metal (hydr) oxides, J. Phys. Chem. B 107 (2003) 9441–9451.
[25] R.G. Lehmann, R.D. Harter, Assessment of copper-soil bond strength by desorption kinetics, Soil Sci. Soc. Am. J. 48 (1984) 769–772.
[26] X.P. Liao, W. Tang, R.Q. Zhou, B. Shi, Adsorption of metal anions of vanadium(V) and chromium(VI) on Zr(IV)-impregnated collagen fiber, Adsorption 14 (2008) 55–64.
[27] S.A. Dean, J.M. Tobin, Uptake of chromium cations and anions by milled peat, Resour. Conserv. Recycl. 27 (1999) 151–156.
[28] R.S. Prakasham, J.S. Merrie, R. Sheela, N. Saswathi, S.V. Ramakrishna, Biosorption of chromium VI by free and immobilized *Rhizopus arrhizus*, Environ. Pollut. 104 (1999) 421–427.
[29] Y. Saĝ, T. Kutsal, Application of adsorption isotherms to chromium adsorption on *Z. ramigera*, Biotechnol. Lett. 11 (1989) 141–144.
[30] D. Park, S. Lim, Y.S. Yun, J.M. Park, Development of a new Cr(VI)-biosorbent from agricultural biowaste, Bioresour. Technol. 99 (2008) 8810–8818.
[31] H. Gao, Y. Liu, G. Zeng, W. Xu, T. Li, W. Xia, Characterization of Cr(VI) removal from aqueous solutions by a surplus agricultural waste—Rice straw, J. Hazard. Mater. 150 (2008) 446–452.
[32] V.K. Gupta, A. Rastogi, Biosorption of hexavalent chromium by raw and acid-treated green alga *Oedogonium hatei* from aqueous solutions, J. Hazard. Mater. 163 (2009) 396–402.
[33] X. Yongjie, H. Haobo, Z. Shujing, Competitive adsorption of copper(II), cadmium(II), lead(II) and zinc(II) onto basic oxygen furnace slag, J. Hazard. Mater. 162 (2009) 391–401.
[34] I. Langmuir, The constitution and fundamental properties of solids and liquids. Part I. Solids, JACS 38 (1916) 2221–2295.
[35] M.H. Kalavathy, L.R. Miranda, *Moringa oleifera*—A solid phase extractant for the removal of copper, nickel and zinc from aqueous solutions, Chem. Eng. J. 158 (2010) 188–199.
[36] H.M.F. Freundlich, Over the adsorption in solution, J. Phys. Chem. 57 (1906) 385–471.
[37] K.S. Tong, M.J. Kassim, A. Azraa, Adsorption of copper ion from its aqueous solution by a novel biosorbent *Uncaria gambir*: Equilibrium, kinetics, and thermodynamic studies, Chem. Eng. J. 170 (2011) 145–153.
[38] M.I. Tempkin, V. Pyzhev, Kinetics of ammonia synthesis on promoted iron catalyst, Acta Phys. Chim. 12 (1940) 327–356.
[39] J.A. Kumar, B. Mandal, Adsorption of Cr(VI) and Rhodamine B by surface modified tannery waste: Kinetic, mechanistic and thermodynamic studies, J. Hazard. Mater. 186 (2011) 1088–1096.
[40] M.M. Dubinin, L.V. Radushkevich, The equation of the characteristic curve of the activated charcoal, Phys. Chem. Sect. 55 (1947) 331–337.
[41] J.R. Gonzalez, J.R.P. Videa, E. Rodriguez, M. Delgado, J.L. Gardea-Torresdey, Potential of *Agave lechuguilla* biomass for Cr(III) removal from aqueous solutions: Thermodynamic studies, Bio. Technol. 97 (2006) 178–182.
[42] F. Helfferich, Ion Exchange, McGraw-Hill, New York, NY, 1962, p. 166.
[43] M. Dakiky, M. Khamis, A. Manassra, M. Mer'eb, Selective adsorption of chromium(VI) in industrial wastewater using low-cost abundantly available adsorbents, Adv. Environ. Res. 6 (2002) 533–540.
[44] Y. Orhan, H. Buyukgungur, The removal of heavy metals by using agricultural wastes, Water Sci. Technol. 28 (1993) 247–255.
[45] M. Jain, V.K. Garg, K. Kadirvelu, Investigation of Cr(VI) adsorption onto chemically treated *Helianthus annuus*: Optimization using response surface methodology, Bioresour. Technol. 102 (2011) 600–605.
[46] A.H. El-Sheikh, M.M. Abu Hilal, J.A. Sweileh, Bioseparation, speciation and determination of chromium in water using partially pyrolyzed olive pomace sorbent, Bioresour. Technol. 102 (2011) 5749–5756.
[47] S. Gupta, B.V. Babu, Removal of toxic metal Cr(VI) from aqueous solutions using sawdust as adsorbent: Equilibrium, kinetics and regeneration studies, Chem. Eng. J. 150 (2009) 352–365.
[48] X.S. Wang, Z.Z. Li, C. Sun, Removal of Cr(VI) from aqueous solutions by low-cost biosorbents: Marine macroalgae and agricultural by-products, J. Hazard. Mater. 153 (2008) 1176–1184.
[49] A. Javaid, R. Bajwa, U. Shafique, J. Anwar, Removal of heavy metals by adsorption on *Pleurotus ostreatus*, Biomass Bioenergy 35 (2011) 1675–1682.
[50] Y. Liu, Is the free energy change of adsorption correctly calculated? J. Chem. Eng. Data 54 (2009) 1981–1985.
[51] S. Lagergren, About the theory of so called adsorption of soluble substances, K. S. Vetenskapsak. Hand. 24 (1898) 1–39.
[52] Y.S. Ho, G. McKay, A comparison of chemisorption kinetic models applied to pollutant removal on various sorbents, Process Saf. Environ. Prot. 76 (1998) 332–340.
[53] Z.Y. Yao, J.H. Qi, L.H. Wang, Equilibrium, kinetic and thermodynamic studies on the biosorption of Cu(II) onto chestnut shell, J. Hazard. Mater. 174 (2010) 137–143.
[54] S.H. Chien, W.R. Clayton, Application of elovich equation to the kinetics of phosphate release and sorption in soils, Soil Sci. Soc. Am. J. 44 (1980) 265–268.
[55] W.J. Weber, J.C. Morris, Kinetics of adsorption on carbon from solution, J. Sanit. Eng. Div. Am. Soc. Civ. Eng. 89 (1963) 31–60.
[56] H. Koyuncu, Adsorption kinetics of 3-hydroxybenzaldehyde on native and activated bentonite, Appl. Clay Sci. 38 (2008) 279–287.
[57] S.J. Allen, G. McKay, K.Y. Khader, Intraparticle diffusion of a basic dye during adsorption onto sphagnum peat, Environ. Pollut. 56 (1989) 39–50.
[58] V.K. Gupta, A.K. Shrivastava, N. Jain, Biosorption of chromium(VI) from aqueous solutions by green algae Spirogyra species, Water Res. 35 (2001) 4079–4085.